Science of Remote Sensing 7 (2023) 100076

Contents lists available at ScienceDirect

Science of Remote Sensing

journal homepage: www.sciencedirect.com/journal/science-of-remote-sensing

Modelling non-linear deforestation trends for an ecological tension zone in Brazil

Vilane Gonçalves Sales

Oeschger Centre for Climate Change Research (OCCR), University of Bern, Switzerland

ARTICLE INFO

Keywords:
Deforestation trends
Generalized additive models
Remote sensing analysis
Ecotonic region
Climatic trends

ABSTRACT

Tropical deforestation is a recent phenomenon that started in the second part of the twentieth century. One may argue that the Brazilian state of Maranhão is an excellent case study for ex-amining deforestation trends and the effects of environmental policies. A man-made line sepa-rates Maranhão into two sections. Due to the administrative divide between the Legal Amazon Maranhão (LM) and the Cerrado Maranhão (CM), one may hypothesize about differences in deforestation between the two regions. This research employs a nonlinear modelling approach based on Generalized Additive Models (GAMs) with a quasi-Poisson distribution and a logarith-mic function to detect deforestation patterns in these areas. Deforestation is linked to the year and a variety of climatic variables. These covariates differ substantially across seasons (rainy and dry) and regions. During times of above-average precipitation, including in the dry and wet seasons, deforestation occurred in the LM area. However, in the non-enforced region, this regime was not followed. According to the statistics, deforestation decreased in the LM region when precipitation levels were below average.

1. Introduction

Tropical deforestation is a relatively recent phenomenon that gained traction in the second half of the twentieth century and was almost entirely confined to tropical regions (Culas, 2014).Tropical dry forests, such as savannas, are among the most endangered and underappreciated forest types on the planet (Bianchi and Haig, 2013). In this regard, the Brazilian Savanna *Cerrado* is arguably the biome that has been most affected by human occupation over the last three decades, owing to increasing pressures for opening up new areas for the production of meat, grains, and ethanol, mostly at the expense of forested areas (MMA, 2018a; Bayma and Sano, 2015). According to the National Institute for Space Research (INPE, 2020), the Cerrado biome lost 6657 km^2 in 2018, a rate equivalent to that observed in the Legal Amazon, a biome twice the size of the Cerrado. This underscores the urgency of the problem, given that the Cerrado habitat is a global hotspot for biodiversity and the birthplace of Brazil's waters.[1]

Almost half of its natural vegetation has been removed (approximately 2 million km), primarily as a result of agricultural expansion. Specifically, between 1990 and 2010, the Cerrado lost 0.6 percent of its natural vegetation every year, owing largely to cattle and large-scale intensive agriculture. This pace of habitat loss equates to over 1700 ha each day, dispersed throughout the Cerrado and the main concern with the progress of deforestation remains in the northern portion of the biome, in states such as Tocantins, Piaui, Bahia, and Maranhão, where the last and largest fragments of natural vegetation remain (Bianchi and Haig, 2013; Francoso et al., 2020).

One could argue that the Brazilian state of Maranhão provides an especially interesting context for studying defor-estation trends and the potential role of environmental policy as observed in Sales et al. (2022). Maranhão is divided into two distinct areas by a man-made line: the Legal Amazon Maranhão (LM) and the Cerrado Maranhão (CM). This division, located approximately 44 west of the meridian, was formed in 1953 to plan the region's economic develop-ment. This scenario provides a unique natural experiment in deforestation in the Legal Amazon Maranhão (LM) and Cerrado Maranhão (CM), because the former has been subject to fundamentally different environmental policies than the latter. More precisely, the tropical forest in the Legal Amazon Maranhão (LM) is subject to a surveillance environ-ment policy called DETER, which uses satellite data to detect deforestation or fire incidents in the region and alerts the environmental agents (IBAMA in Portuguese) to fine responsible individuals (IBAMA, 2017). The surveillance

E-mail addresses: vilane.g.sales@gmail.com, vilane.goncalves@unibe.ch.

[1] The Legal Amazon is an area that corresponds to 59% of the Brazilian territory and encompasses all eight states (Acre, Amapá, Amazonas, Mato Grosso, Pará, Rondônia, Roraima and Tocantins) and part of the State of Maranhão (west of the meridian Of 44°W), totalling more than 5 million km^2 (IPEA, 2008).

https://doi.org/10.1016/j.srs.2023.100076
Received 25 May 2022; Received in revised form 19 October 2022; Accepted 8 January 2023
Available online 16 January 2023

environment policy, on the other hand, was inapplicable to the Maranhão state's other biomes until 2018.

Using this spatial division, one can speculate on the deforestation variations between the Legal Amazon Maranhão and the Cerrado Maranhão. To form deforestation patterns, this article uses a nonlinear modelling approach based on Generalized Additive Models (GAMs) with a quasi-Poisson distribution and logarithmic relation function. The decision to use non-linear modelling for this task is based on prior research indicating that the majority of ecological and climatic data reflect complex relationships and that non-linear models, such as GAMs, may be especially well suited to capture confounding effects in trends (Bio et al., 1998; Bell et al., 2015; Auderset Joye and Rey-Boissezon, 2015; Lusk et al., 2016; Pourtaghi et al., 2016; Halperin et al., 2016, de Souza et al., 2017; Antunez et al., 2017; Liu et al., 2018; Moreno-Fernandez et al., 2018).

A recent research indicated that GAMs have been successfully used to explore climate and fire relationships which is an indicative of deforestation/degradation episode (Abatzoglou et al., 2018). However, non-linear models were found to be used sparingly to examine deforestation. For instance, Chaves et al. (2008) demonstrated that deforestation affected disease incidence in Cuba. Additionally, a binomial GAM model was used to represent both forest and habitat destruction in Tanzania's Eastern Arc Mountains protected areas Green et al. (2013). Bebber and Butt (2017) examined the impact of protected areas on global carbon emissions in America, Africa, and Asia in 2017. And, Mendes and Junior (2012) studied deforestation, corruption, and economic growth in the Legal Amazon region of Brazil. To date, this paper is the first to attempt to examine deforestation patterns for the ecological tension zone in the state of Maranhão (CM and LM) using generalized additive models.

2. Materials and methods

2.1. Study area

Maranhão, whose indigenous name translates as *'flowing river'* (Girardi, 2015), is one of the ten largest states in Brazil, covering an area of more than 330 thousand square kilometres. A contact region of nearly 21,228 km^2 resides in the centre of Maranhão, where a mosaic of savanna physiognomies sits alongside ombrophilous woodland formations (open and dense forest). This region is known as the Maranhão Ecological Tension Zone (ETZ), and it is characterised by a convergence zone with a mix of open and closed formations, each of which supports unique and numerous organisms, resulting in a high level of biodiversity (Rossatto et al., 2013). Additionally, the artificial line runs across the centre of Maranhão's Ecological Tension Zone. This paper's research area spans a buffer of 50k km^2 to the west and east of the political line and comprises approximately 21 municipalities. The study includes only municipalities divided by the 1953 line of demarcation (approximately 44 west of the meridian). Importantly, the agencies, rules, legislation, and practises at the state level are the same for both areas. Fig. 1 depicts the delineation. According to the geographical characteristics and vegetation cover of the state of Maranhão, the ETZ has two distinct seasons: between November and April, the rainy season is described by partly cloudy to cloudy skies and an increase in air humidity, which dampens the thermal sensation and peaks in March, and the dry season, which starts in May and runs until the end of October with its peak around August. The area is characterised by a humid-dry or savanna climate that is warm and tropical (Aw). Temperatures are high, with yearly averages above 25 °C, and reaching 28 °C in the examined region's southeast. Annual precipitation ranges from 1000 mm peaking at 1700 mm on the plateaus. Average levels of the climatic variable for both areas can be found in the Supplementary Information file **S1**.

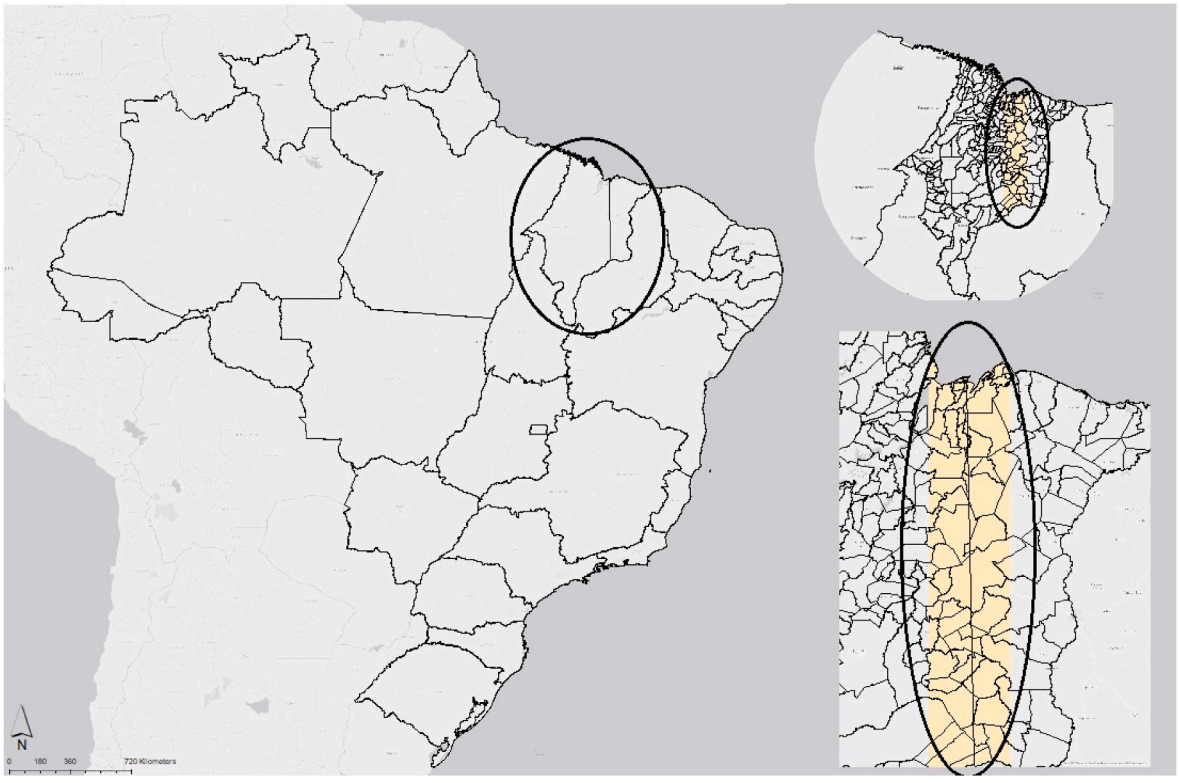

Fig. 1. Map of Maranhão Study Area The map indicates the location of the state of Maranhao and the institutional delimitation. The vertical line express the institutional division of the Legal Amazon in the State and the light yellow demarcation shows the studied region which is equivalent to 50 km buffer east (CM) and west (LM). Map created by author with data from MMA (2018b); NUGEO (2018); EMBRAPA (2018). (For interpretation of the references to colour in this figure legend, the reader is referred to the Web version of this article.)

The national environmental policy provides policies specific to different regions of Brazil creating programs and action plans. In order to control for degradation of the forest by selective logging and forest fires, the government uses the DETER program which is part of the Action Plan for the Prevention and Control of Deforestation in the Legal Amazon (PPCDAm in Portuguese). The DETER (the Legal Amazon forest Change survey) program has been conducted by the National Institute of Spatial Research (INPE in Portuguese) using data from Terra's MODIS sensor since May 2004 with a spatial resolution of 250 m. DETER was established to assist environmental officers in combatting illegal deforestation. This device can detect changes in forest cover larger than 25 ha. Detection cannot account for cloud cover. The lower sensor resolution is offset by the system's regular observation capability, making DETER an ideal tool for notifying inspection bodies of new changes. DETER is a regular process that creates five-day deforestation warning maps after the MODIS picture is acquired. (INPE-DETER, 2018; Diniz et al., 2015). There was an interesting note in the DETER alerts: The notifications were only applied to the part of Maranhão within the Legal Amazon boundaries, leaving the rest of the state outside of the evaluation and range.

2.2. Remote sensing data

Two remotely sensed datasets were used – Vegetation Indices 16-Day L3 Global 250 m MODIS13Q1 and Land Cover Type Yearly L3 Global 500 m MODIS12Q1. This paper utilised the MODIS Land Cover Type Product (MCD12Q1) with the classification scheme of the University of Maryland (UMD). A complete list of the classes and their defini-tions can be found in Setiawan et al. (2014); Sulla-Menashe and Friedl (2018a). The MODIS Vegetation Indices (VI) (MOD13Q1) product consists of time series comparisons of global vegetation conditions that can be used to monitor the Earth's terrestrial change detection. The two vegetation indices derived from the product are the Normalized Dif-ference Vegetation Index (NDVI) (Rouse et al., 1974) and the Enhanced Vegetation Index (EVI) (Huete et al., 1994, 1997). To optimise the vegetation signal and minimise atmospheric effect and soil background noise, the EVI index has been reported to be more responsive to canopy structural variations including canopy type:

$$EVI = \frac{\rho_{NIR} - \rho_{red}}{\rho_{NIR} + C_{1\rho_{red}} - C_{2\rho_{blue}} + L}(G) \quad (1)$$

where p_{red} and p_{NIR} and p_{blue} are the reflectance in the bands 1,2 and 3 from MODIS sensor, C_1 and C_2 are atmospheric resistance coefficients, and L and G are the canopy background adjustment and the gain factor, respec-tively. The coefficients adopted for the MODIS EVI algorithm are, $L = 1$, $C_1 = 6$, $C_2 = 7.5$ and $G = 2.5$ (Huete et al., 1997). Ratana et al. (2005) note that this index is sufficiently stable to permit meaningful comparisons of seasonal, inter-annual, and long-term variations of vegetation structure, phenology, and biophysical parameters.

From January 2001 to December 2016, a total of 368 images of the Vegetation Index (EVI) product MOD13Q1 and 16 images of the Land Cover product MCD12Q1 were downloaded, along with their respective auxiliary data such as quality check (QC) and quality assurance (QA), which provide a summary of the pixel quality. The images were smoothed in the TIMESAT programme which is useful for presenting noise generated by the presence of clouds during the satellite's transit (Jönsson and Eklundh, 2004). The programme implements three smoothing algorithms: dual logistics, Savitzky-Golay, and asymmetric Gaussian. Borges et al. (2014) observed that double logistics worked better for MODIS EVI data from Brazilian Cerrado. Double logistics is a function that is both harmonic and polynomial. Equation (2) expresses it mathematically

$$g(t; x_1, ..., x_4) = \frac{1}{1 + \exp\left(\frac{x_1 - t}{x_2}\right)} - \frac{1}{1 + \exp\left(\frac{x_3 - t}{x_4}\right)} \quad (2)$$

where x_1 denotes the direction of the left inflection point and x_2 denotes the rate of transition. The parameter x_3 specifies the location of the right-side inflection point, while x_4 specifies the rate of change at that point (Bayma and Sano, 2015). The double logistics filter was used to smooth the initial average values of EVI for each formation per pixel from 2001 to 2016.

In order to perform the analysis, the smoothed EVI images were imported onto MATLAB and scaled to the valid range of −0.2 to 1. Two images per month for each year were uploaded - excluding October and November during leap years because they had only one image within the month. According to the VI User Guide, the VI Quality Assessment band for each scene was converted to unsigned16bit and used to create a Goodness mask to exclude pixels with clouds and not produced for other reasons than clouds (Didan et al., 2015). Before filtering the EVI scenes with the Goodness mask, it was necessary to condition EVI starting values to a specific threshold so to avoid values not related to the denominated transitional forest. The criterion was taken following Geerken (2009) parameters to characterise forest in a transitional biome. Following that, the EVI index scenes were selected based on threshold values and only EVI values with good quality according to the Goodness mask were maintained after cloud coverage was removed.

With the Land Cover product MCD12Q1 it was required to resize and interpolate each image to the corresponding sizes of EVI images. The interpolation method utilised followed a deterministic method called Nearest Neighbourhood (NN) or Thiessen method. The nearest method was considered because there is no extrapolation of the data, which would not have been suitable for categorical data and because it showed to be the fastest computation method with modest memory requirements (Sluiter, 2012). After the interpolation a land cover mask was produced to select only pixels in the images presenting forest classification according to the University of Maryland classification Sulla--Menashe and Friedl (2018b).Forests with less than 40% tree cover were removed from the analysis because they do not accurately represent a transitional forest primarily associated with the Cerrado biome (Bayma and Sano, 2015). Finally, to ensure compliance within each month, values of EVI of the first image (16 first days of the month) were compared to the second image (16 remaining days of the month). In this sense, the final scene/image presents pixels assuming the highest quality and no cloud coverage. At the end of the process, pixels were selected within the 50 km buffer measured departing from the artificial Legal Amazon line to the west and east portions of the State. The approach above was undertaken for all the images corresponding and EVI values for each month of each year, giving 192 final image results. For the leap year, the process stopped at the land cover mask filtering process. Deforestation thresholds were established for each vegetation structure considered in the smoothed time series images according to Bayma and Sano (2015) methodology. The term "deforestation threshold" refers to the EVI values at which defor-estation/disturbance can be assumed. Due to the high degree of seasonality observed in Maranhao studied region, the EVI time series of natural areas follow a generally sinusoidal pattern; their lowest values roughly correspond to the height of the dry season, while their highest values roughly correspond to the peak of the rainy season. When a natural environment is deforested, the vegetation indices of subsequent MODIS sensor passages usually fall below the deforestation thresholds (Bayma and Sano, 2015).

To determine whether pixels were deforested, the dataset was aggregated to the annual level, resampled, and com-pared to the Brazilian Annual Land Use and Land Cover Mapping Project (MapBiomas Collection 5) dataset. The MapBiomas dataset categorises deforestation according to the following criteria:

$$Suppression_t = \begin{cases} F_{t-2} \\ F_{t-1} \\ A_t \\ A_{t+1} \end{cases} \quad (3)$$

where F corresponds to Forest as a class of vegetation (Forest

Formation, Savanic Formation), A corresponds to any class of Anthropic use and t = 2000, …, 2016 taking 2000 as the base year. When a pixel was classified as "Forest" for at least two years and then "Anthropic" for at least two years, the algorithm considered it to be part of a deforestation episode (Souza et al., 2020; MapBiomas, 2021). The final dataset consisted of sum of monthly EVI pixels signalled as deforested for 192 images over 16 years.

2.3. Climate covariates

The climatic covariates used to examine deforestation patterns were collected from the National Meteorological Institute's Meteorological Database for Teaching and Research (BDMEP – INMET in Portuguese), which contains historical series for many typical meteorological stations in the INMET station network (BDMEP, 2018). Each con-ventional weather station (see Table 1) is composed of several remote sensors that continuously record meteorological parameters (e.g., temperature, precipitation, humidity, and solar radiation), which are then annotated by an observer and sent to a collection centre. To derive the climate dataset, it was collected monthly average maximum temperature (*maMxT*), monthly average minimum temperature (*maMinT*), monthly average precipitation (*maP*), monthly average relative humidity (*maRH*) and number of hours of sunlight in a month as total solar radiation (*maTS*) from January 2001 to December 2016.

A post-process analysis was carried to ensure that there were no gaps in the data for the climatic variables. The first step was to transform all of the data to a tabular format, which means that all variables were stored in one table and positions were defined as latitude, longitude, and elevation values. Following localising the x,y,z coordinates, each shapefile was developed. The shapefiles were picked and extracted by month. Next, an interpolation approach was applied to areas with no results. The method of choice was ordinary kriging, which has been argued as the best interpolation technique for sparse data (Sluiter, 2012). Ordinary kriging is an example of a probabilistic approach that includes the principle of randomness. Kriging uses a linear combination of the calculated quantities and the spatial similarity between the data to compute the weights. Intrinsic stationary is assumed due to the uncertain mean. The climatic data set are rarely stationary, so this assumption might fail. To overcome this issue it was used different sizes and shapes of neighbourhood to adjust the kriging ordinary model (Sluiter, 2012). Finally, the files were resampled to the scale of the EVI index.

Generally, for temperature, precipitation, and other climate data, the best way to interpret and study these phe-nomenons is using anomaly measurements, which correspond to the difference between a measurement and mean (Kawale et al., 2011). In this sense, the average value of the variable of each image for each month was computed, giving a total of 192 images analysed for both regions (CM and LM), and for each climatic variable, a total of 1224 images. Following this procedure, the number of pixels with values higher and lower than the average value of the variable was extracted to a table. Finally, the table included the total of pixels with values greater than or less than the mean for each variable, which translated into ten variables. All the data that support the findings of this study are available in the referenced sites above.

Table 1
Meteorological stations in the ecological tension zone - study region.

Station ID	Lat	Long	Altitude	Name	Area
82571	−5.5	−45.23	153	Barra do Corda	LM
82970	−9.5	−46.2	285	Alto Parnaiba	LM
82460	−4.21	−44.76	25	Bacabal	LM
82765	−7.33	−47.46	193	Carolina	LM
82376	−3.26	−45.65	45	Ze Doca	LM
82476	−4.86	−43.35	104	Caxias	CM
82382	−3.73	−43.35	104	Chapadinha	CM
82676	−6.03	−44.25	180	Colinas	CM
82280	−2.53	−44.21	51	Sao Luis	CM

2.4. Deforestation trends and climatic factors - generalized additive models

A number of studies on land cover change examine the rates and dynamics of environmental transition in terms of their primary factors (Van Vliet et al., 2013; Almeida et al., 2016; Sonter et al., 2017). More precisely, these studies seek to identify the primary drivers of land-cover change across a variety of geographical and historical contexts. Several studies show that drier, flatter, more fertile areas with adequate drainage and therefore more agriculturally suitable areas are more likely to be cleared (Kaimowitz and Angelsen, 1998; Grimaldi et al., 2014). By contrast, it has been reported that poor soil quality contributes to relatively high deforestation rates, as insufficient soil endowment accelerates clearing for other purposes, such as pasture (Geist and Lambin, 2001; Silva Costa et al., 2012; Fujisaki et al., 2015; Laurent et al., 2021).

Environmental factors and biophysical drivers are increasingly being recognised as being fundamental to defor-estation, not just a contributing factor (Geist and Lambin, 2001). For example, Barni et al. (2015) demonstrated that.

the areas affected by forest fires were dependent on forest type and climate factors, regardless of the rate and magnitude of deforestation. Ecotone-influenced zones are more deforested than other factors, i.e., the denser the forest, the less deforested it is. Additionally, the highest frequency of forest fires was observed during *El Nino* events in areas with economic influence, such as the state of Maranhão. Additionally, they discovered that the areas most affected by forest fires throughout the research period were connected with severe climatic events and that fires occurred more frequently in ecotone-influenced zones (Barni et al., 2015). These findings strongly imply that it is critical to account for climate factors in ecotone zones when examining deforestation trends.[2]

Considering that a significant percentage of ecological and climatic data sets do not agree with the conclusions underlying a linear regression model, a generalized additive model (GAM) can overcome this issue. The mathemat-ical modelling technique utilises smooth functions to capture the impact of predicted variables (Larsen, 2015). The generalized additive model (GAM) with an exponential family distribution has been the most widely used method for measuring and quantifying the non-linear relationship between phenology and covariates such as meteorological con-ditions, primarily because it allows for non-parametric adjustment of non-linear seasonality and trend effects (Bio et al., 1998; Bell et al., 2015; Auderset Joye and Rey-Boissezon, 2015; Lusk et al., 2016; Pourtaghi et al., 2016; Halperin et al., 2016, 2016de Souza et al., 2017; Antunez et al., 2017; Liu et al., 2018; Moreno-Fernandez et al., 2018).

Given the nature of the dataset, the deforestation counts are often estimated using an overdispersed Poisson regres-sion model. A GAM with a quasi-poisson distribution and a logarithmic connection is used to quantify forest distur-bance as a proxy for deforestation. The quasi-poisson distribution is appropriate for this study because the variance of the deforestation variable is significantly greater than the mean, which is a characteristic of ecological data (Zuur, 2011). The quasi model formulation has the advantage of preserving natural, interpretable parameters and enabling standard model diagnostics without sacrificing efficient fitting algorithms. The model assumes that $Y_i \sim$ Poi μ_i, *0*

where the mean μ_i for the i th observation vary as a function of the covariates for that observation (Ver Hoef and Boveng, 2007; Rodrigues et al., 2019). Because the mean $\mu_i > 0$, it is natural to model:

[2] In this study, ecological tension zone, ecotone zones and transitional forest have the same meaning.

$$g(\mu_i) = \alpha + \sum_{j=1}^{J} s_j(x_{ij};\beta_j) + \sum_{k=1}^{K} \gamma_k u_{ik} \quad (4)$$

where $\mu_i = E(Y)$ and is a monotonic link function. The functions s_j denotes the smooth function for variables.

x_j while y_k is the parameter estimate for the linear relationship of variables, u_k and μ_i.

The equation considered the sum of EVI pixels signalled as deforested ($Def_{(EV\ I\bar{I})}$) and several covariates cal-culated as the total amount of positive and negative anomaly pixels. A variable's anomaly is its deviation from the

climatological normal. The normal is a baseline number that is the long-term average of the same variable. In this study, a (t) positive anomaly indicates that the value of the variable was higher than the baseline value and a (!) neg-ative means a lower value compared to the mean. It also included Year as a smooth function variable to allow the observance of the trend throughout the studied period. Model selection followed the forwarding approach of Zuur et al. (2014), p.391, with two distinct models chosen for each area (CM and LM). An autocorrelation examination was performed after model choice, but none of the models proved to be autocorrelated. The model began with a GAM with a single covariate, then fitted 13 separate versions using a variety of different smoothers (penalised splines "ps," cubic splines "cr," and cyclic splines "cc") and contrasted their quasi-Akaike knowledge criterion (quasi-AIC) (Burn-ham and Anderson, 2010). The model with the lowest value was elected as the main model and then it was fitted to 12 different models, each with the addition of the variable with the lowest quasi-AIC. The forward selection stopped at the moment the main model had the lowest quasi-AIC value comparing to the remaining models. The choice of smoothing parameters for smoothing splines in GAM should always be accompanied by a graphical verification of functional associations with the outcome to verify clinical plausibility (Moore et al., 2011). The final model shows

$$Def_{(EV\ I_i)} = \alpha + f_{Year}(Year_i) + f_{maP}(\uparrow\downarrow \mathrm{maP}_i) + f_{\mathrm{maMxT}}(\downarrow \mathrm{maMxT}_i) + f_{\mathrm{maMinT}}(\uparrow\downarrow \mathrm{maMinT}_i) + f_{maRH}(\uparrow\downarrow maRH_i) + f_{maTS}(\downarrow maTS_i) + \in_i \quad (5)$$

where a is an intercept parameter, the f are smooth functions, and the e_i are independent N 0, cr random vari-ables. To visualise the results graphically, the first derivative of the trend splines derived from the deforestation data was generated using the Generalized Additive Model (GAM). The grey band represents a 95% confidence interval for simultaneous point-wise observations. This graph may be used to determine whether the rate of deforestation is growing or reducing statistically substantially. The strategy is to compute the fitted trend's first derivatives using the finite difference method. To get derivatives using finite differences, we calculated the values of the fitted trend on a grid of points encompassing the whole data set. After then, the grid was shifted slightly to recompute the trend values at the new places. The differences between the two fitted sets of data indicate the trend's initial differences and serve as a proxy for the trend's slope at any point in time.

For handling spatial datasets, ArcMap 10.4.1, ArcPy 10.4.1, and the extensions Geostatistical Analyst, Spatial Analyst and Spatial Statistics from ArcToolbox (ESRI, 2016b,b), and MATLAB R2017a with Statistics and Machine Learning and Image Processing Toolbox (MATLAB, 2017) was extensively used. For statistical analysis and mod-elling, R (R Core Team, 2018) and several packages specially 'MASS'(Venables and Ripley, 2002), 'mgcv' (Wood, 2004; 2004, 2011, 2017), 'MuMIn' (Barton, 2020) and 'gratia' (Simpson, 2018) were considered.

2.5. Validation

To validate the results on the EVI time series a confusion matrix was employed. The two-by-two output table comprises four binary classifier outputs. The confusion matrix indicates how many observations were made in each cell. The uncertainty matrix's rows correspond to the real class and its columns to the expected class. Diagonal and off-diagonal cells, respectively, refer to correctly categorised and incorrectly classified observations (Lewis and Brown, 2001). A confusion matrix was produced for the dataset after resampling to the spatial resolution of the MapBiomas dataset and aggregating to year maps.

The covariates were validated using cross-validation processes during the interpolation procedure. Cross-validation uses all the data to estimate the trend and autocorrelation models. It removes each data location one at a time and predicts the associated data value. This is also known as leaving-one-out, and can be computed for all or a subset of the data locations (ESRI, 2016b). In the kriging method, the cross-validation produced other results that helped evaluate the best interpolation method. More specifically, the Average Standard Errors (ASE) and Root Mean Square Standardized Error (RMSE) were computed.

In terms of statistics, after the model selection phase, model validation with additive modelling was visual rather than numerical. Four diagnostic plots were examined, including a Q-Q plot and histogram of model residuals, a plot of residuals vs the linear predictor, and a plot of observed vs fitted values. An important assumption of the analysis is that the buffer zone, created either side of the artificial line to isolate and compare pixels, is geographically and biologically homogeneous. To find support for this important assumption an effect size index for the two areas either side of the line was first calculated. Following Cohen (1977), differences in the means, expressed in terms of the pooled within areas standard deviation, is calculated.

3. Results

The validation results showed that the algorithm to detect deforestation had an accuracy superior to 95% which tells what proportion of the data points was predicted correctly. The classification results can be found in the supplementary file **S1**. In addition, for the covariates analyses, ASE were on average 95% of the value of the RMSE, proving to be a reasonable interpolation method with valid results. The resulting Cohen index is interpreted in terms of the average percentile standing area relative to another. This result is an index with a value of 0.2 which indicates that the mean of one area is at the 58th percentile of the buffer zone, i.e the dissimilarities for the two areas are close to zero. Since the chosen buffer zone may seem somewhat arbitrary, the next step was to examine whether forests between the two regions differ just outside of the chosen buffer zone. More precisely, areas 0.2° just outside buffer zone on each side of the two regions were isolated and their difference was similarly tested. The corresponding Cohen index was 0.59, which is at the 69th percentile, and thus one can reject the null hypothesis that there is no difference between these two regions. As a matter of fact, the index value of 0.59 indicates a difference of 33% in the two distributions.

All the analysis was based on generalized additive models (GAM). Figures A1 to A.6 in the Appendix provide diagnostic graphs. The baseline model includes the sum of the number of pixels deforested from 192 monthly obser-vations of EVI values changing over the years with the five influencing covariates (Precipitation, Max Temperature, Min Temperature, Sunlight and Humidity) considering the Legal Amazon

Table 2
Results of a Generalized Additive Model for Maranhão State - Cerrado Maranhão (CM) and Legal Maranhão (LM) and when different seasons are considered (Dry and Rain).

Region	Quasi-AIC	R-squared Adjusted	Deviance Explained
Legal Maranhão (LM)	196.361	0.584	64.4%
Legal Maranhão (LM) Rain Season	186.201	0.927	90.3%
Legal Maranhão (LM) Dry Season	169.434	0.922	89.6%
Cerrado Maranhão (CM)	207.489	0.936	84.4%
Cerrado Maranhão (CM) Rain Season	179.184	0.995	97.8%
Cerrado Maranhão (CM) Dry Season	138.754	0.984	93.2%

line. Table 2 summarises the diagnostic outcomes, including deviation, Quasi-AIC, and R-squared. The best model for the Legal Maranhão is the one that de-picts the dry season with the lowest Quasi-AIC value and the maximum power of deviance explanation. In the Cerrado Maranhão, the best model is the dry season model with the lowest Quasi-AIC score although the rain Season model presented the maximum power of deviance explanation.

The best way to understand and interpret GAMs is through visual representation as cited in Zuur et al. (2014). The output models depicted in Figs. 2–7 are named according to the location (CM and LM) and season (Dry and Rain). It is possible to check for the path of deforestation through the years and the climatic state during that period plotting the smoothing functions. The results are shown regarding to the average number of pixels of the covariates. The signs ! and t refer to the sum of the number of negative and positive pixels deviation to the mean, respectively.

Beginning with the Cerrado Maranhão (CM) region, deforestation is generally associated with precipitation changes and rising temperatures, as indicated in Fig. 2. On average, deforestation occurred throughout the rainy season, which lasts from November to April, during periods of reduced rainfall and warming temperatures (see Fig. 3). De-forestation was associated with more precipitation and cooler temperatures during the dry season. Additionally, Fig. 4 illustrates how deforestation rose dramatically between 2004 and 2016, peaking in 2016 during the dry season.

Figs. 5–7 demonstrate how deforestation behaved on average over the research period in Legal Maranhão (LM). Deforestation occurred, according to the baseline model presented in Fig. 5, during periods of decreasing relative humidity, decreased maximum temperatures, and increased precipitation levels. When split down into sea-sons, the pattern becomes more obvious. Fig. 6 shows how deforestation occurred throughout the raining season. The positive changes in the curves related with deforestation are few. During periods of increasing precipitation and warmth, it is feasible to notice a minor yet positive effect of deforestation. For the dry season, Fig. 7 illustrates that deforestation was related to changes in the temperature and increased humidity. In contrast to the non-enforced region.

deforestation was not associated with increased rainfall. Low levels of deforestation, on the other hand, were related with low amounts of precipitation during the examined season.

It is possible to examine how policy implementation has impacted the route of deforestation throughout time. Fig-ures6 and 7 demonstrate a distinct downward trend beginning in 2004 and an increasing trend at the end of the research period. Between 2008 and 2012, deforestation was negative, but increased in the years that followed. Additionally, deforestation occurred with constant rainfall in general, but was consistently positive and rising with severe precipitation events. The interacted climatic variables are available in the supplementary file **S1**.

4. Discussion

The GAMs verified that deforestation is connected to yearly variation

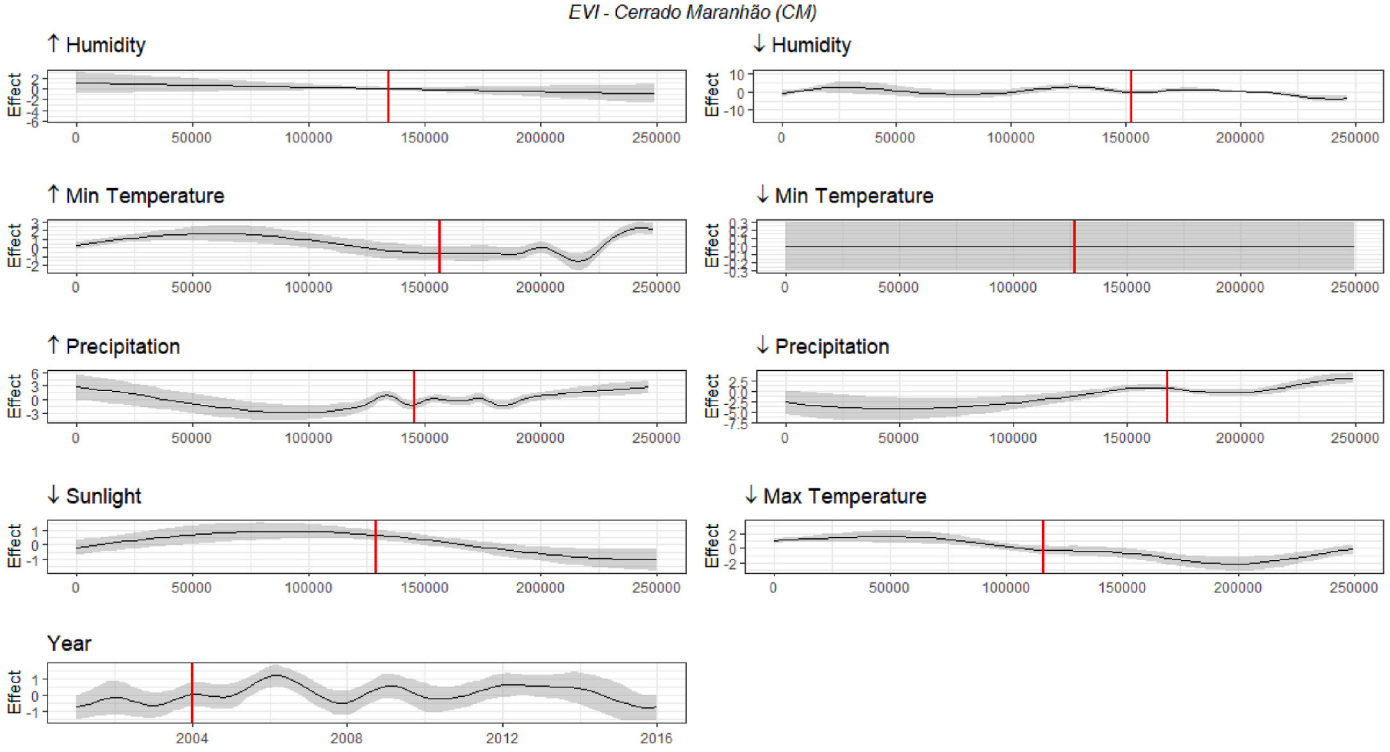

Fig. 2. Model EVI Maranhão Cerrado (CM). Model Maranhão Cerrado using EVI values. The red vertical line indicates the averages of the sample. Showing graphical representation of significant covariates. The red vertical line for the covariate Year indicates the beginning of the surveillance policy. (For interpretation of the references to colour in this figure legend, the reader is referred to the Web version of this article.)

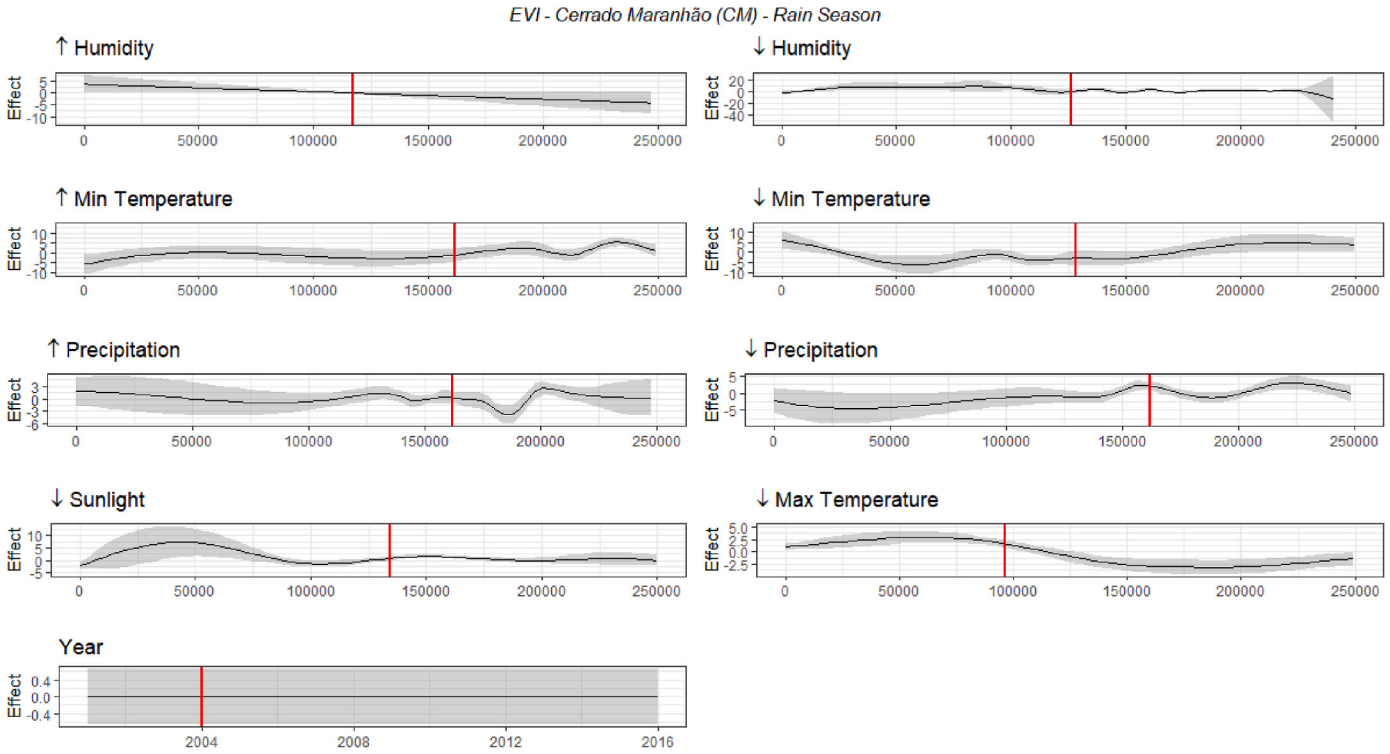

Fig. 3. Model EVI Maranhão Cerrado (CM) - Rain Season. Model Maranhão Cerrado using EVI values. The red vertical line indicates the averages of the sample. Showing graphical representation of significant covariates.The red vertical line for the covariate Year indicates the beginning of the surveillance policy. (For interpretation of the references to colour in this figure legend, the reader is referred to the Web version of this article.)

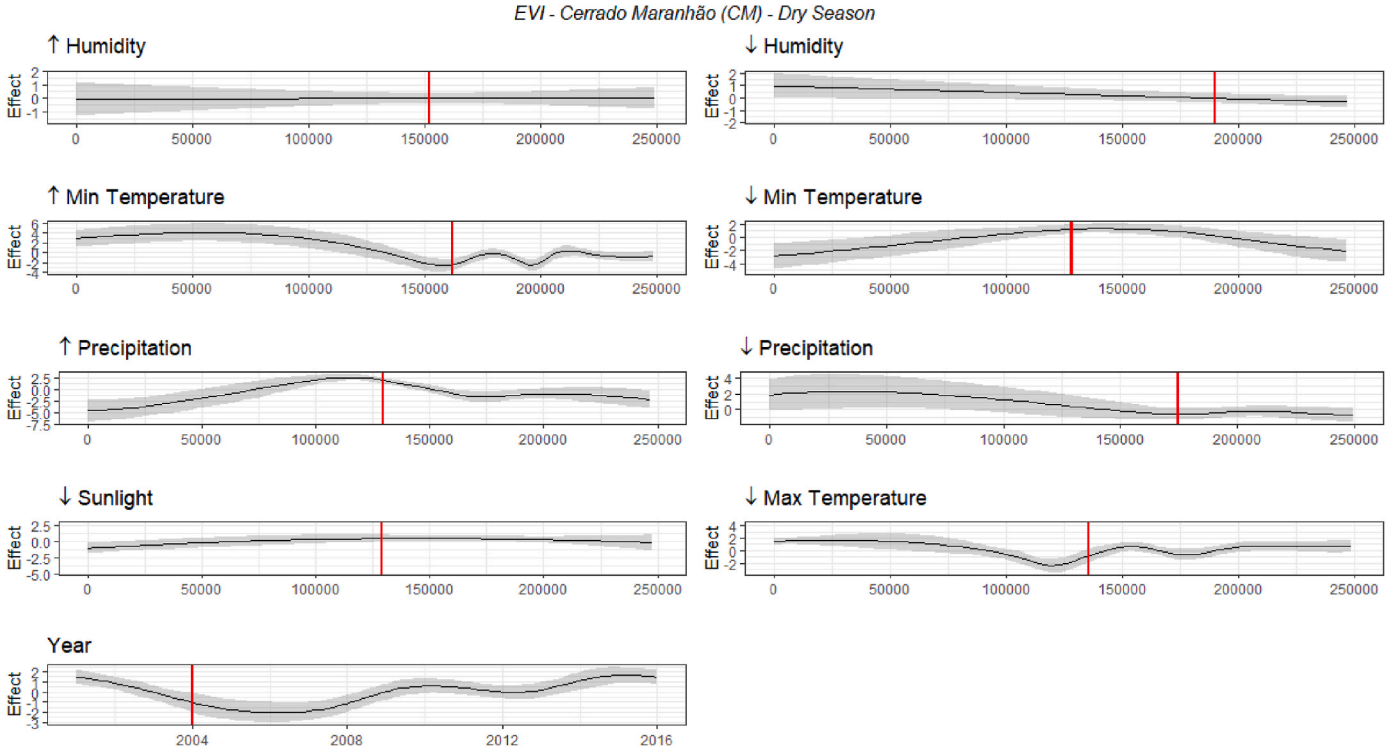

Fig. 4. Model EVI Maranhão Cerrado (CM) - Dry Season. Model Maranhão Cerrado using EVI values. The red vertical line indicates the averages of the sample. Showing graphical representation of significant covariates. (For interpretation of the references to colour in this figure legend, the reader is referred to the Web version of this article.)

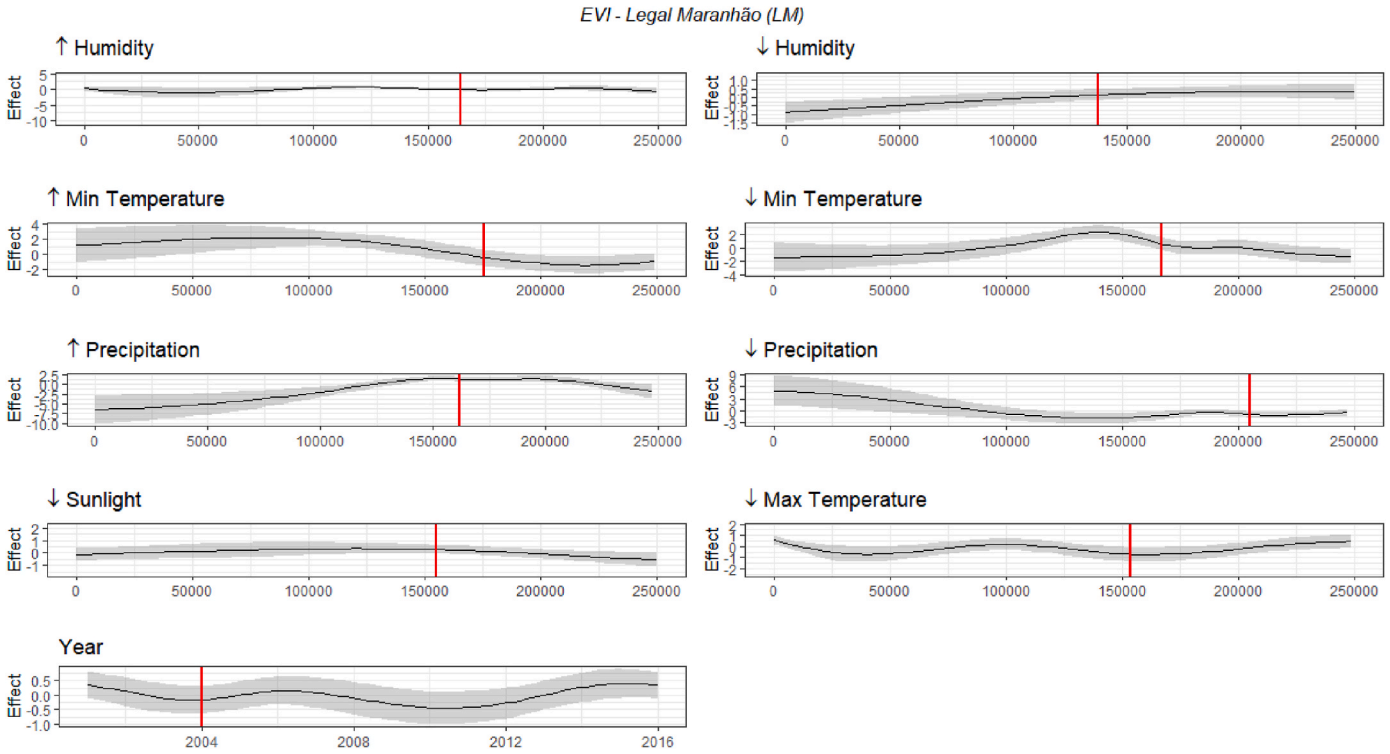

Fig. 5. Model EVI Legal Maranhão (LM). Model Legal Maranhão using EVI values. The red vertical line indicates the averages of the sample. Showing graphical representation of significant covariates.The red vertical line for the covariate Year indicates the beginning of the surveillance policy. (For interpretation of the references to colour in this figure legend, the reader is referred to the Web version of this article.)

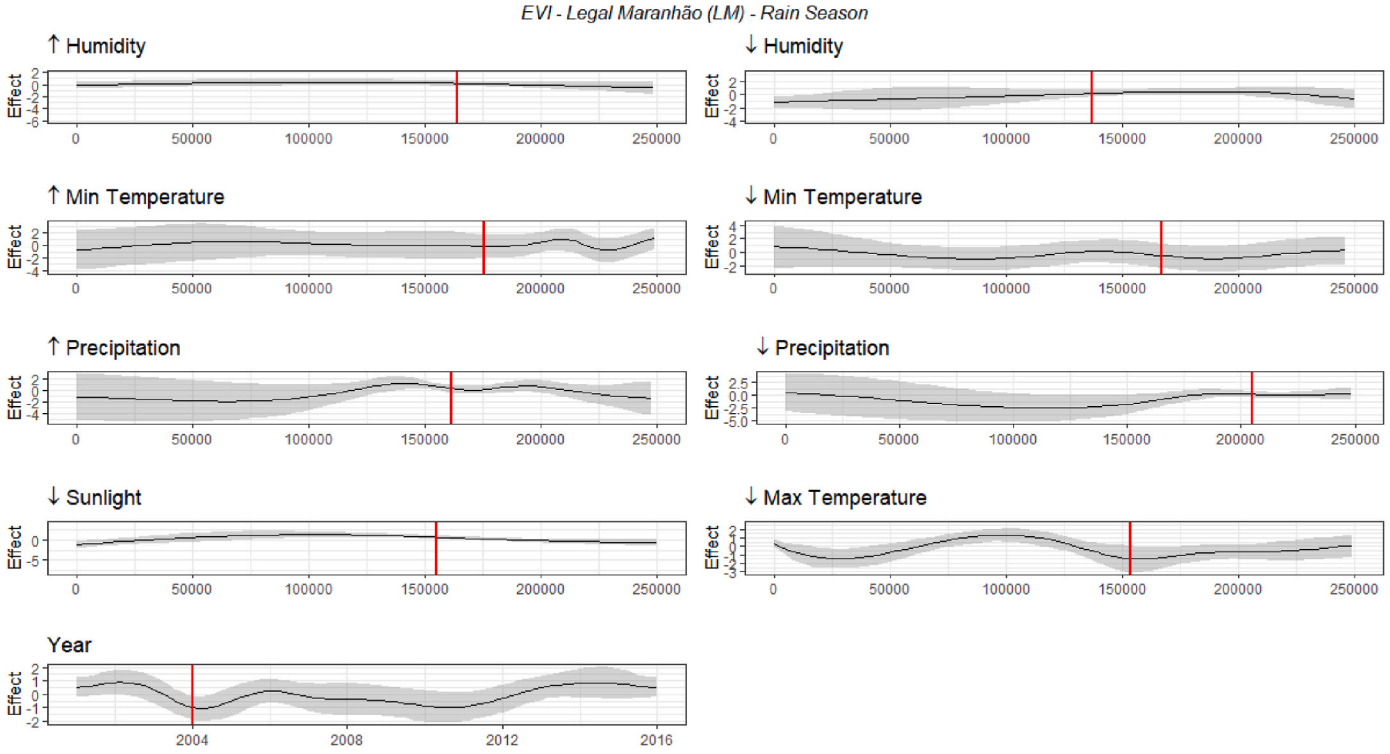

Fig. 6. Model EVI Legal Maranhão (LM) - Rain Season. Model Legal Maranhão using EVI values. The red vertical line indicates the averages of the sample. Showing graphical representation of significant covariates.The red vertical line for the covariate Year indicates the beginning of the surveillance policy. (For interpretation of the references to colour in this figure legend, the reader is referred to the Web version of this article.)

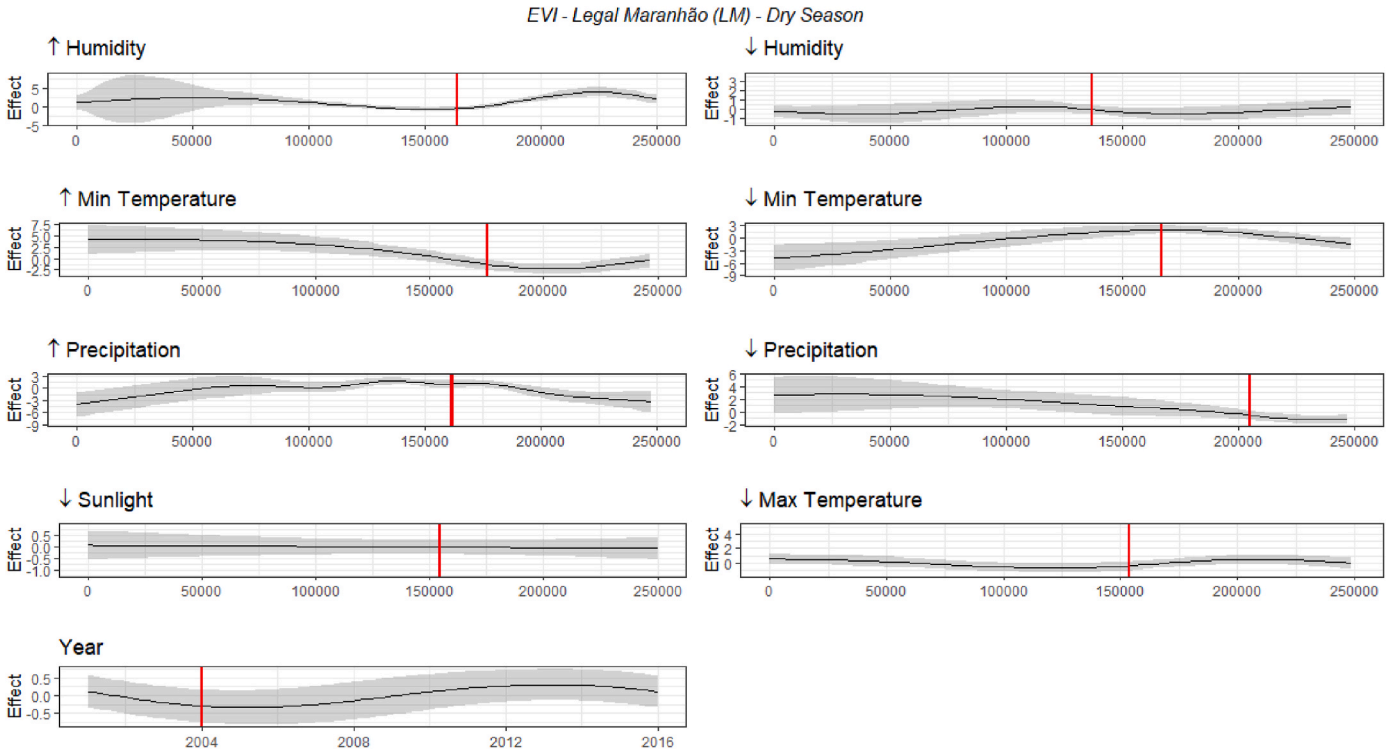

Fig. 7. Model EVI Legal Maranhão (LM) - Dry Season. Model Legal Maranhão using EVI values. The red vertical line indicates the averages of the sample. Showing graphical representation of significant covariates.The red vertical line for the covariate Year indicates the beginning of the surveillance policy. (For interpretation of the references to colour in this figure legend, the reader is referred to the Web version of this article.)

and climatic variables, but they also demon-strated that there are significant differences in trends across seasons and between the LM and CM regions. In summary, the best description of the deforestation climatic situation for the Legal Maranhão comprises significant amounts of precipitation. During the dry season, low levels of deforestation was related to low levels of precipitation. For the Cerrado Maranhão, deforestation is generally related to changes in the precipitation and rising temperatures. More specifically, during the rainy season, deforestation increased with lower levels of precipitation and the dry season showed how deforestation increased with increasing rainfall.

Given that the majority of deforestation happens as a result of human activity, the deforestation oscillation process is driven by individual choices. However, the results indicate that most of this activity occurred differently in the two areas. As previously stated, the LM area is subject to an environmental monitoring programme (DETER) that use satellite images to identify deforestation in tropical and transitional forest and penalises anyone found to be responsible. In this regard, the deforestation patterns in the monitored region indicate that deforestation occurred during periods of heavy precipitation, showing that the presence of rain as a proxy for clouds in satellite images complicates the identification of vegetation changes. Precipitation levels above average may suggest the presence of clouds acting as natural barriers.

Additionally, deforestation in the two locations behaved differently throughout the dry season. Given that CM and LM have the same biophysical properties and weather patterns (for comparisons of climatic variables, see supplemen-tary file **S1**). It is possible to see that deforestation rose in one of the zones - the unsupervised one - during periods of intense rainfall. Human activity may have changed away from dry seasons marked by bright skies and toward raining periods marked by cloudy days. In other words, implementation plans at environmental monitoring impacted human behaviour. Following this pattern closely, Müller et al. (2020); Menegassi (2020) also describe how deforestation al-legedly increased during the rainy season of January to April 2020 in the Legal Amazon, which contradicts the widely held belief that the rainy season is a quiet period for logging in the Legal Amazon, given the logistical difficulties inherent in operating logging equipment in the rain (Müller et al., 2020).

Furthermore, it looks as though there is a spillover impact from environmental enforcement in the LM zone to the CM region. One credible piece of evidence is that deforestation continued in the Cerrado Maranhão during both seasons with different cycles. Throughout the dry season, when there was heavy rainfall, deforestation rose as opposed to the LM region. However, it looks as if there is no spillover impact from environmental regulation in the LM area to the CM area as can be seen that deforestation continued in the Cerrado Maranhão increasing through the years or it showed a linear relationship (raining season).

There are of course a number of limitations to the analysis undertaken here. Following Murase et al. (2009) approach, possible errors in modelling could be taken into account. First of all, in terms of predicting the trend of deforestation based on a list of variables, the model implicitly assumes that the predicted range or potential space is fully occupied by forest, which in reality might not be true. Additionally, the spatial distribution of the vegetation indices may exhibit dynamic behaviour over time, so that a potential area may or may not be sparsely vegetated for a certain period (e.g., during sampling) due to progressive succession of forest. Or a temporary absence could be due to natural causes, such as, attack of pests or diseases or inter-species competition. Secondly, the current presence of forest reflects the contexts of the past which in turn could give rise to uncertainty (though on a smaller scale) in predicting the environment. Also, the regional environmental conditions follow changing trends of different duration, so it is possible that in certain cases an observed value may be declining due to regional changes rather local changes, but the prediction model was not able to detect this dynamic behaviour. Additionally, the study was based on coarse image resolution which could neglect local changes in the sample area. The results could also feasibly suffer from overfiting since more data is needed to optimise the smoothing algorithms. Finally, our results may not be generalizable to other areas, such as dense tropical forest and

open fields.

5. Conclusion

One may argue that the Brazilian state of Maranhão is a particularly intriguing case study for examining defor-estation patterns and the possible influence of environmental policies. An artificial line divides Maranhão into two different regions. Using this geographic distinction, one might hypothesize on the differences in deforestation between the Legal Amazon Maranhão and the Cerrado Maranhão. This paper employed a nonlinear modelling technique based on Generalized Additive Models (GAMs) with a quasi-Poisson distribution and logarithmic connection function to generate deforestation patterns in the Legal Maranhão and the Cerrado Maranhão. The approach indicated that year and climatic covariates are connected to deforestation, although these varied widely across seasons and areas. Defor-estation occurred in the Legal Maranhão area during periods of excessive precipitation, which were above average. Cerrado Maranhão, during the dry season, there was a significantly divergent course of deforestation in the Legal Maranhão region. Indeed, the data reveal that the Cerrado Maranhão area had an increasing trend when precipitation levels were above average. Increased precipitation may indicate the existence of clouds functioning as natural barriers to the monitoring policy in the LM region. Human activity may have moved away from dry seasons marked by bright and clear skies and toward rainy seasons marked by cloudy days. In other words, regulations aimed at environmental monitoring changed deforestation patterns.

CRediT authorship contribution statement

Conceptualization of this study, Methodology, Data Curation, Software, Formal analysis, Investigation, Writing- Original Draft, Writing-Review Editing, and Visualization.

Declaration of competing interest

The authors declare the following financial interests/personal relationships which may be considered as potential competing interests: Vilane G. Sales reports financial support was provided by Coordination of Higher Education Personnel Improvement.

Data availability

Data will be made available on request.

Acknowledgements

We thank Laisa G. Sales for useful software and technical support. This article is the result of the research project funded by the Coordination of Superior Level Staff Improvement in Brazil. CAPES BEX 2228/15-7.

Appendix A. Supplementary data

Supplementary data to this article can be found online at https://doi.org/10.1016/j.srs.2023.100076.

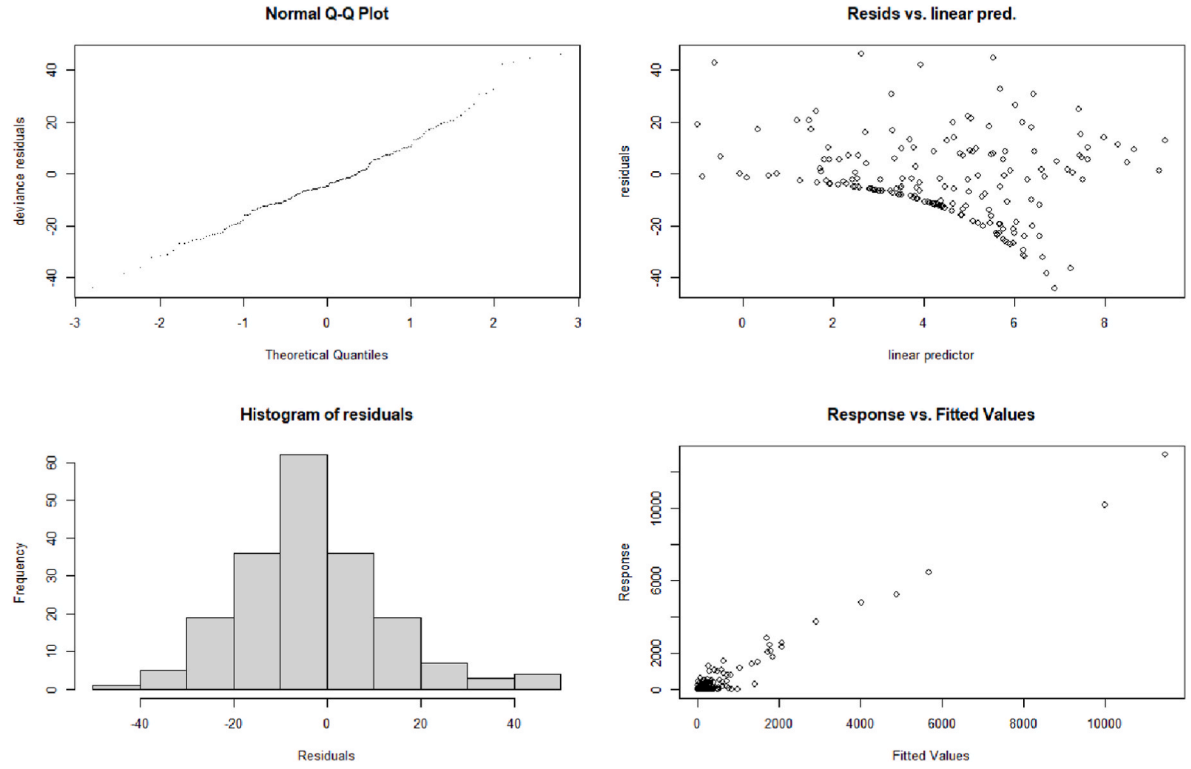

Fig. A.1. The result of Cerrado Maranhão (CM) model. Each array shows four diagnostics plots, including a Q-Q plot (top left) and histogram (bottom left) of model residuals, a plot of residuals vs the linear predictor (top right), and a plot of observed vs fitted values.

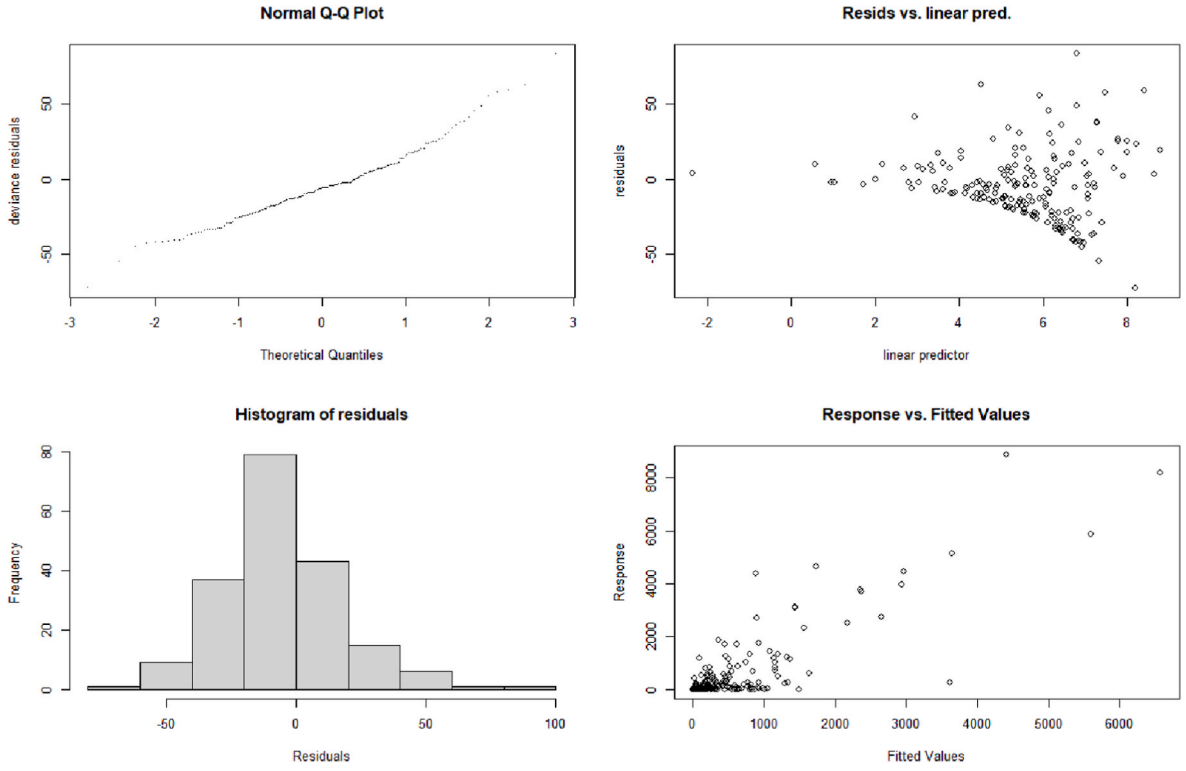

Fig. A.2. The result of Legal Maranhão (LM) model. Each array shows four diagnostics plots, including a Q-Q plot (top left) and histogram (bottom left) of model residuals, a plot of residuals vs the linear predictor (top right), and a plot of observed vs fitted values.

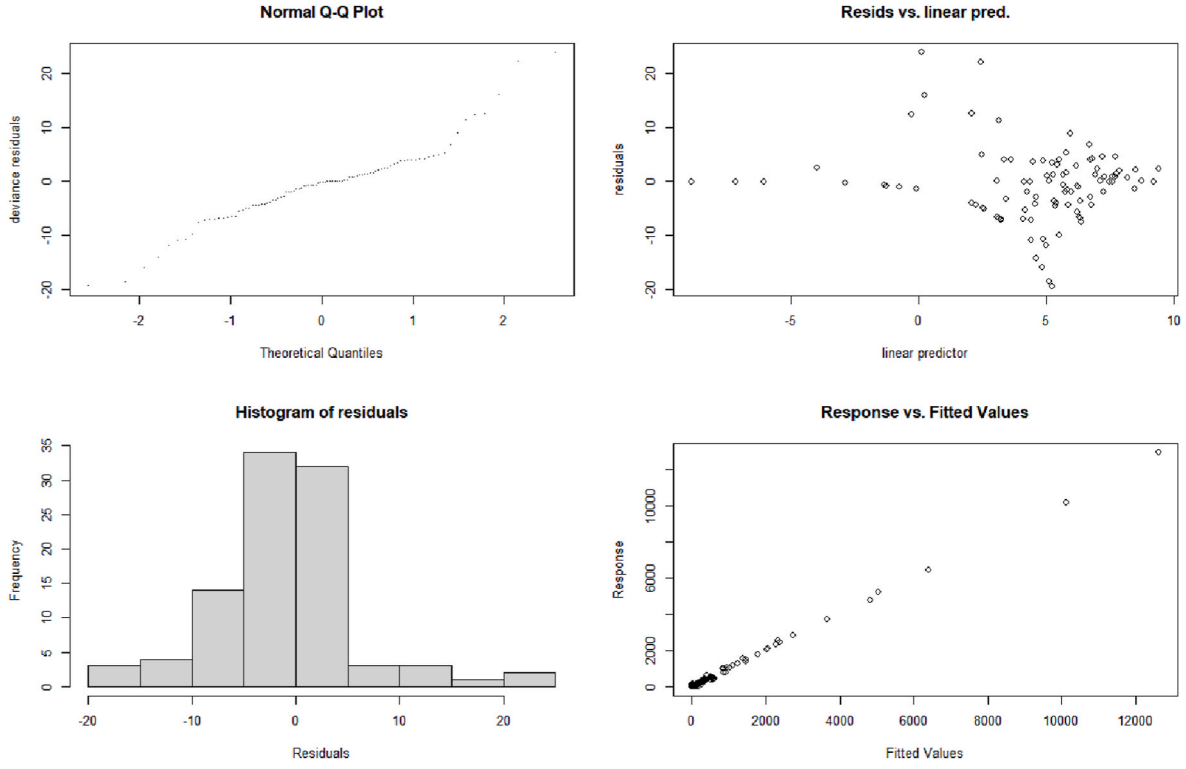

Fig. A.3. The result of Cerrado Maranhão Rain Season (CM) model. Each array shows four diagnostics plots, including a Q-Q plot (top left) and histogram (bottom left) of model residuals, a plot of residuals vs the linear predictor (top right), and a plot of observed vs fitted values.

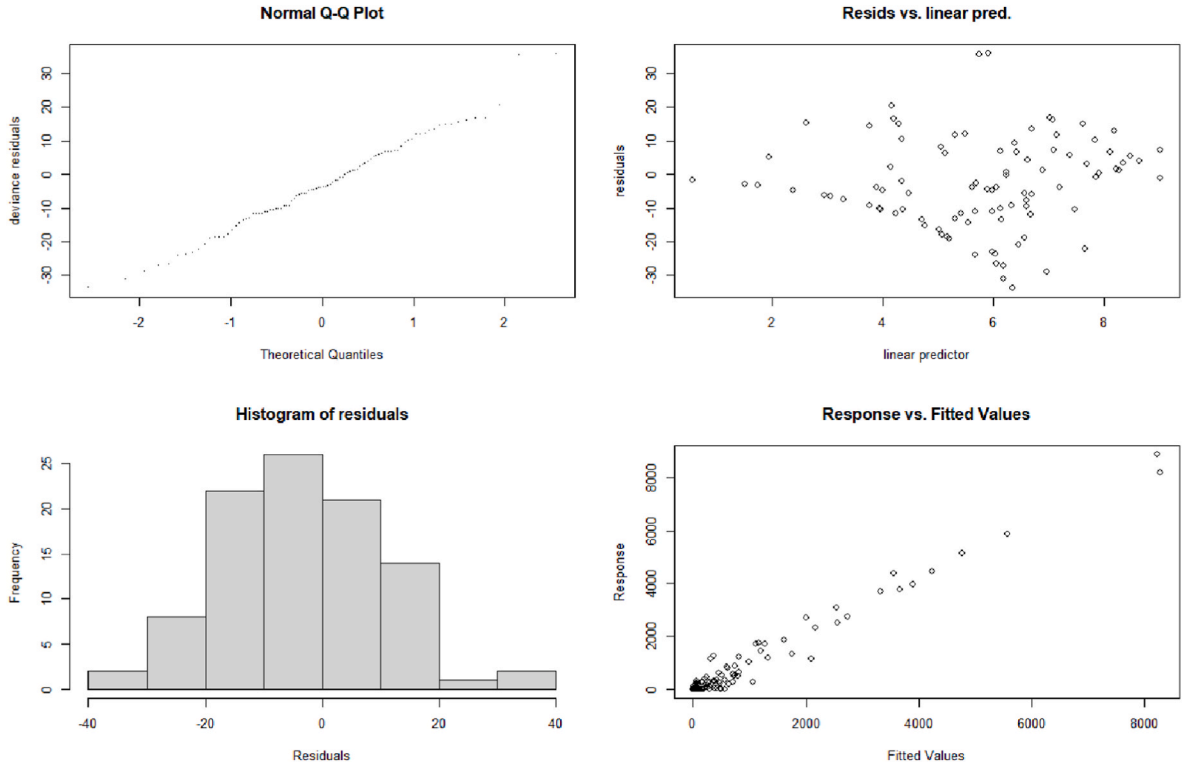

Fig. A.4. The result of Legal Maranhão Rain Season (LM) model. Each array shows four diagnostics plots, including a Q-Q plot (top left) and histogram (bottom left) of model residuals, a plot of residuals vs the linear predictor (top right), and a plot of observed vs fitted values.

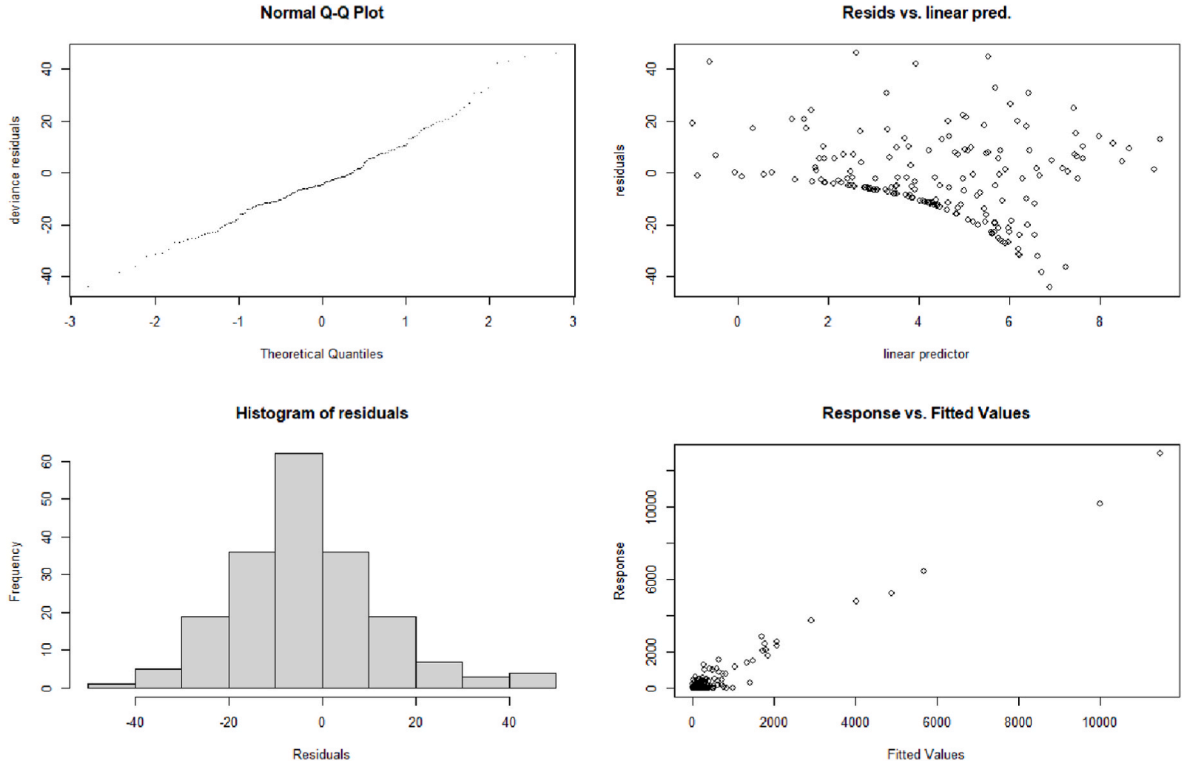

Fig. A.5. The result of Cerrado Maranhão Dry Season (CM) model. Each array shows four diagnostics plots, including a Q-Q plot (top left) and histogram (bottom left) of model residuals, a plot of residuals vs the linear predictor (top right), and a plot of observed vs fitted values.

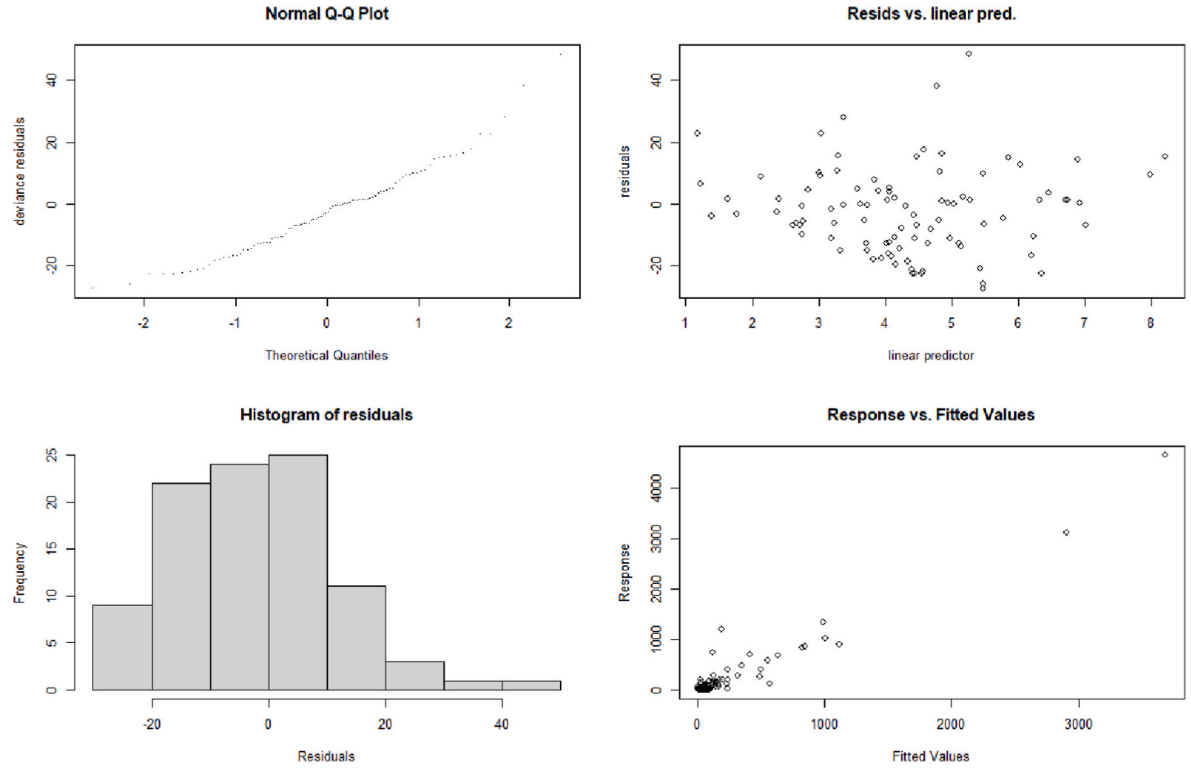

Fig. A.6. The result of Legal Maranhão Dry Season (LM) model. Each array shows four diagnostics plots, including a Q-Q plot (top left) and histogram (bottom left) of model residuals, a plot of residuals vs the linear predictor (top right), and a plot of observed vs fitted values.

References

Abatzoglou, J.T., Williams, A.P., Boschetti, L., Zubkova, M., Kolden, C.A., 2018. Global patterns of interannual climate–fire relationships. Global Change Biol. 24, 5164–5175.

Almeida, C.A.d., Coutinho, A.C., Esquerdo, J.C.D.M., Adami, M., Venturieri, A., Diniz, C. G., Dessay, N., Durieux, L., Gomes, A.R., 2016. High spatial resolution land use and land cover mapping of the brazilian legal amazon in 2008 using landsat-5/tm and modis data. Acta Amazonica 46, 291–302.

Antunez, P., Hernandez-Diaz, J., Wehenkel, C., Clark-Tapia, R., 2017. Generalized models: an application to identify environmental variables that significantly affect the abundance of three tree species. Forests 8, 59. https://doi.org/10.3390/f8030059.

Auderset Joye, D., Rey-Boissezon, A., 2015. Will charophyte species increase or decrease their distribution in a changing climate? Aquat. Bot. 120, 73–83. https://doi.org/10.1016/j.aquabot.2014.05.003.

Barni, P.E., Pereira, V.B., Manzi, A.O., Barbosa, R.I., 2015. Deforestation and forest fires in Roraima and their relationship with phytoclimatic regions in the Northern Brazilian Amazon. Environ. Manag. 55, 1124–1138. https://doi.org/10.1007/s00267-015-0447-7.

Barton, K., 2020. MuMIn: multi-model inference. https://CRAN.R-project.org/package=MuMIn. r package version 1.43.17.

Bayma, A.P., Sano, E.E., 2015. Series temporais de indices de vegetacao (ndvi e evi) do sensor modis para deteccao de desmatamentos no bioma cerrado. Bol. Ciências Geodésicas 21, 797–813. https://doi.org/10.1590/s1982-21702015000400047.

BDMEP, 2018. Bdmep - banco de dados meteorologicos para ensino e pesquisa do inmet. http://www.inmet.gov.br/projetos/rede/pesquisa/.

Bebber, D.P., Butt, N., 2017. Tropical protected areas reduced deforestation carbon emissions by one third from 2000012. Sci. Rep. 7 https://doi.org/10.1038/s41598-017-14467-w.

Bell, T.W., Cavanaugh, K.C., Reed, D.C., Siegel, D.A., 2015. Geographical variability in the controls of giant kelp biomass dynamics. J. Biogeogr. 42, 2010–2021. https://doi.org/10.1111/jbi.12550.

Bianchi, Carlos A., Haig, S.M., 2013. Deforestation trends of tropical dry forests in central Brazil. Biotropica 45, 395–400. https://doi.org/10.1111/btp.12010, 10.1111/btp.12010.

Bio, A., Alkemade, R., Barendregt, A., 1998. Determining alternative models for vegetation response analysis: a non-parametric approach. J. Veg. Sci. 9, 5–16. https://doi.org/10.2307/3237218.

Borges, E.F., Sano, E.E., Medrado, E., 2014. Radiometric quality and performance of TIMESAT for smoothing moderate resolution imaging spectroradiometer enhanced vegetation index time series from western Bahia State, Brazil. J. Appl. Remote Sens. 8, 083580, 10.1117/1.JRS.8. 083580. http://remotesensing.spiedigitallibrary.org/article.aspx?doi=10.1117/1.JRS.8.083580.

Burnham, K.P., Anderson, D.R., 2010. In: Model Selection and Multimodel Inference: a Practical Information-Theoretic Approach. 2. Springer, New York, NY. OCLC: 846443242.

Chaves, L.F., Cohen, J.M., Pascual, M., Wilson, M.L., 2008. Social exclusion modifies climate and deforestation impacts on a vector-borne disease. PLoS Neglected Trop. Dis. 2, 1–8. https://doi.org/10.1371/journal.pntd.0000176, 10.1371/journal.pntd.0000176.

Cohen, J., 1977. Statistical power analysis for the behavioral sciences. In: Cohen, J. (Ed.), Statistical Power Analysis for the Behavioral Sciences. Academic Press, pp. 1–17. https://doi.org/10.1016/B978-0-12-179060-8.50006-2. http://www.sciencedirect.com/science/article/pii/B9780121790608500062.

Culas, R.J., 2014. Causes of deforestation and policies for reduced emissions (redd+): a cross-country analysis. IUP J. Appl. Economic. 13, 7–27. http://search.proquest.com/docview/1630008843?accountid=8630.

de Souza, J.B., Reisen, V.A., Franco, G.C., Ispány, M., Bondon, P., Santos, J.M., 2017. Generalized additive models with principal component analysis: an application to time series of respiratory disease and air pollution data. J. Roy. Stat. Soc.: Series C (Applied Statistics) 67, 453–480. https://doi.org/10.1111/rssc.12239.

Didan, K., Munoz, A.B., Solano, R., Huete, A., 2015. Modis Vegetation Index User's Guide (Mod13 Series) - Version 3.00 - Collection 6. NASA EOSDIS LP DAAC, 10. 5067/MODIS/MOD13Q1.006. https://lpdaac.usgs.gov/dataset_discovery/modis/modis_products_table/mod13q1_v006.

Diniz, C.G., Souza, A.A.d.A., Santos, D.C., Dias, M.C., Luz, N.C.d., Moraes, D.R.V.d., Maia, J.S., Gomes, A.R., Narvaes, I.d.S., Valeriano, D.M., Maurano, L.E.P., Adami, M., 2015. Deter-b: the new amazon near real-time deforestation detection system. IEEE J. Sel. Top. Appl. Earth Obs. Rem. Sens. 8, 3619–3628. https://doi.org/10.1109/JSTARS.2015.2437075.

Embrapa, 2018. A embrapa - portal embrapa. Environmental Systems Research Institute. https://www.embrapa.br/. ESRI, 2016a. ArcMap.

ESRI, 2016. ArcPy. http://resources.arcgis.com/en/help/main/10.4.1/index.html#//000v000000v7000000.

Francoso, R.D., Dexter, K.G., Machado, R.B., Pennington, R.T., Pinto, J.R., Brandao, R.A., Ratter, J.A., 2020. Delimiting floristic biogeographic districts in the cerrado and assessing their conservation status. Biodivers. Conserv. 29, 1477–1500.

Fujisaki, K., Perrin, A.S., Desjardins, T., Bernoux, M., Balbino, L.C., Brossard, M., 2015. From forest to cropland and pasture systems: a critical review of soil organic carbon stocks changes in amazonia. Global Change Biol. 21, 2773–2786.

Geerken, R.A., 2009. An algorithm to classify and monitor seasonal variations in vegetation phenologies and their inter-annual change. ISPRS J. Photogrammetry Remote Sens. 64, 422–431. https://doi.org/10.1016/j.isprsjprs.2009.03.001.

Geist, H.J., Lambin, E.F., 2001. In: What Drives Tropical Deforestation, 4. LUCC Report series, p. 116.

Girardi, G., 2015. Sem dúvida. http://revistagalileu.globo.com/Galileu/0,6993, ECT498531-1716-5,00.html.
Green, J.M., Larrosa, C., Burgess, N.D., Balmford, A., Johnston, A., Mbilinyi, B.P., Platts, P.J., Coad, L., 2013. Deforestation in an african biodiversity hotspot: extent, variation and the effectiveness of protected areas. Biol. Conserv. 164, 62–72. https://doi.org/10.1016/j.biocon.2013.04.016.
Grimaldi, M., Oszwald, J., Dolédec, S., del Pilar Hurtado, M., de Souza Miranda, I., De Sartre, X.A., De Assis, W.S., Castaneda, E., Desjardins, T., Dubs, F., et al., 2014. Ecosystem services of regulation and support in amazonian pioneer fronts: searching for landscape drivers. Landsc. Ecol. 29, 311–328.
Halperin, J., LeMay, V., Coops, N., Verchot, L., Marshall, P., Lochhead, K., 2016. Canopy cover estimation in miombo woodlands of Zambia: com- parison of landsat 8 oli versus rapideye imagery using parametric, nonparametric, and semiparametric methods. Remote Sens. Environ. 179, 170–182. https://doi.org/10.1016/j.rse.2016.03.028.
Huete, A., Justice, C., Liu, H., 1994. Development of vegetation and soil indices for modis-eos. Remote Sens. Environ. 49, 224–234.
Huete, A., Liu, H., Batchily, K., Van Leeuwen, W., 1997. A comparison of vegetation indices over a global set of tm images for eos-modis. Remote Sens. Environ. 59, 440–451.
IBAMA, 2017. Instituto Brasileiro do Meio Ambiente e dos Recursos Naturais Renovaveis. http://www.ibama.gov.br/Online. (Accessed 1 August 2017).
INPE, 2020. Instituto Nacional de Pesquisas Espaciais - National Institute for Spatial Research. http://www.inpe.br/ingles/Online. (Accessed 1 December 2020).
Inpe-Deter, 2018. Deter — coordenaçao-geral de observaçao da terra. http://www.obt.inpe.br/OBT/assuntos/programas/amazonia/deter.
IPEA, 2008. O que e Amazonia legal? http://www.ipea.gov.br/desafios/index.php?option=com_content&id=2154:catid=28& Itemid=23 Online. (Accessed 2 March 2016).
Jönsson, P., Eklundh, L., 2004. Timesat—a program for analyzing time-series of satellite sensor data. Comput. Geosci. 30, 833–845. https://doi.org/10.1016/j.cageo.2004.05.006. https://www.sciencedirect.com/science/article/pii/S0098300404000974.
Kaimowitz, D., Angelsen, A., 1998. Economic Models of Tropical Deforestation. CIFOR.
Kawale, J., Chatterjee, S., Kumar, A., Liess, S., Steinbach, M.S., Kumar, V., 2011. Anomaly Construction in Climate Data: Issues and Challenges. CIDU, pp. 189–203.
Larsen, K., 2015. Gam: the Predictive Modelling Silver Bullet. Unpublished.
Laurent, F., Poccard-Chapuis, R., Plassin, S., Piketty, M.G., Hasan, A.F., Messner, F., Osis, R., Perrier, F., Huang, L.Z., 2021. Drought sensitivity of pastures related to soil and landform in the eastern amazon. J. Appl. Remote Sens. 15, 024514.
Lewis, H., Brown, M., 2001. A generalized confusion matrix for assessing area estimates from remotely sensed data. Int. J. Rem. Sens. 22, 3223–3235.
Liu, X., Song, Y., Yi, W., Wang, X., Zhu, J., 2018. Comparing the random forest with the generalized additive model to evaluate the impacts of outdoor ambient environmental factors on scaffolding construction productivity. J. Construct. Eng. Manag. 144, 04018037 https://doi.org/10.1061/(asce)co.1943-7862.0001495.
Lusk, C.H., McGlone, M.S., Overton, J.M., 2016. Climate predicts the proportion of divaricate plant species in New Zealand arborescent assemblages. J. Biogeogr. 43, 1881–1892. https://doi.org/10.1111/jbi.12814.
MapBiomas, P., 2021. MATLAB, 2017. MATLAB. The MathWorks Inc. https://mapbiomas.org/en.
Mendes, C.M., Junior, S.P., 2012. Deforestation, economic growth and corruption: a nonparametric analysis on the case of amazon forest. Appl. Econ. Lett. 19, 1285–1291. https://doi.org/10.1080/13504851.2011.619487, 10.1080/13504851.2011.619487, arXiv.
Menegassi, D., 2020. Desmatamento na amazônia atinge nível recorde no primeiro trimestre de 2020. O)) eco 13.
Mma, 2018a. Governo divulga desmatamento no cerrado. MMA - assessoria de Comunicaçao Social. http://www.mma.gov.br/index. php/comunicacao/agencia-informma?view=blog&id=3066.
MMA, 2018b. Ministério do meio ambiente. http://www.mma.gov.br/Online. (Accessed 8 January 2017).
Moore, L., Hanley, J.A., Turgeon, A.F., Lavoie, A., 2011. A comparison of generalized additive models to other common modeling strategies for continuous covariates: implications for risk adjustment. J. Biometric. Biostatic. https://doi.org/10.4172/2155-6180.1000109, 02.
Moreno-Fernandez, D., Augustin, N.H., Montes, F., Cañellas, I., Sánchez-González, M., 2018. Modeling sapling distribution over time using a functional predictor in a generalized additive model. Ann. For. Sci. 75 https://doi.org/10.1007/s13595-017-0685-3.
Müller, C., et al., 2020. Brazil and the amazon rainforest. www.europarl.europa.eu/RegData/etudes/IDAN/2020/648792/IPOL_IDA (2020) 648792_EN.pdf.
Murase, H., Nagashima, H., Yonezaki, S., Matsukura, R., Kitakado, T., 2009. Application of a generalized additive model (gam) to reveal rela- tionships between environmental factors and distributions of pelagic fish and krill: a case study in sendai bay, Japan. ICES (Int. Counc. Explor. Sea) J. Mar. Sci. 66, 1417–1424. https://doi.org/10.1093/icesjms/fsp105.
NUGEO, 2018. http://www.nugeo.uema.br/.
Pourtaghi, Z.S., Pourghasemi, H.R., Aretano, R., Semeraro, T., 2016. Investigation of general indicators influencing on forest fire and its suscepti- bility modeling using different data mining techniques. Ecol. Indicat. 64, 72–84. https://doi.org/10.1016/j.ecolind.2015.12.030.
R Core Team, 2018. R: A Language and Environment for Statistical Computing. R Foundation for Statistical Computing, Vienna, Austria. https://www.R-project.org/.
Ratana, P., Huete, A.R., Ferreira, L., 2005. Analysis of cerrado physiognomies and conversion in the modis seasonal-temporal domain. Earth Interact. 9, 1–22. https://doi.org/10.1175/1087-3562(2005)009<0001:aocpac>2.0.co;2.
Rodrigues, M., Santana, P., Rocha, A., 2019. Effects of extreme temperatures on cerebrovascular mortality in Lisbon: a distributed lag non- linear model. Int. J. Biometeorol. 63, 549–559, 10.1007/s00484-019-01685-2. http://link.springer.com/10.1007/s00484-019-01685-2.
Rossatto, D.R., Hoffmann, W.A., de Carvalho Ramos Silva, L., Haridasan, M., Sternberg, L.S.L., Franco, A.C., 2013. Seasonal variation in leaf traits between congeneric savanna and forest trees in central Brazil: implications for forest expansion into savanna. Trees (Berl.) 27, 1139–1150. https://doi.org/10.1007/s00468-013-0864-2.
Rouse, J.W., Haas, R.H., Schell, J.A., Deering, D.W., et al., 1974. Monitoring Vegetation Systems in the Great Plains with Erts, vol. 351. NASA special publication, p. 309.
Sales, V.G., Strobl, E., Elliott, R.J., 2022. Cloud cover and its impact on Brazil's deforestation satellite monitoring program: evidence from the cerrado biome of the brazilian legal amazon. Appl. Geogr. 140, 102651.
Setiawan, Y., Yoshino, K., Prasetyo, L.B., 2014. Characterizing the dynamics change of vegetation cover on tropical forestlands using 250m multi- temporal modis evi. Int. J. Appl. Earth Obs. Geoinf. 26, 132–144. https://doi.org/10.1016/j.jag.2013.06.008.
Silva Costa, L.G., Miranda, I.S., Grimaldi, M., Silva, M.L., Mitja, D., Lima, T.T.S., 2012. Biomass in different types of land use in the Brazil's arc of deforestation. For. Ecol. Manag. 278, 101–109. https://doi.org/10.1016/j.foreco.2012.04.007.
Simpson, G.L., 2018. gratia: ggplot-based graphics and other useful functions for GAMs fitted using mgcv. https://github.com/gavinsimpson/gratia r package version 0.1-0.
Sluiter, R., 2012. Interpolation Methods for the Climate Atlas. KNMI.
Sonter, L.J., Herrera, D., Barrett, D.J., Galford, G.L., Moran, C.J., Soares-Filho, B.S., 2017. Mining drives extensive deforestation in the brazilian amazon. Nat. Commun. 8, 1–7.
Souza, C.M., Shimbo, Z., Rosa, J., M.R, Parente, L.L., A. Alencar, A., Rudorff, B.F.T., Hasenack, H., Matsumoto, M., G. Ferreira, L., Souza- Filho, P.W.M., de Oliveira, S. W., Rocha, W.F., Fonseca, A.V., Marques, C.B., Diniz, C.G., Costa, D., Monteiro, D., Rosa, E.R., Vélez-Martin, E., Weber, E.J., Lenti, F.E.B., Paternost, F.F., Pareyn, F.G. C., Siqueira, J.V., Viera, J.L., Neto, L.C.F., Saraiva, M.M., Sales, M.H., Salgado, M.P. G., Vasconcelos, R., Galano, S., Mesquita, V.V., Azevedo, T., 2020. Reconstructing three decades of land use and land cover changes in brazilian biomes with landsat archive and earth engine. Rem. Sens. 12, 10.3390/rs12172735. https://www.mdpi.com/2072-4292/12/17/2735.
Sulla-Menashe, D., Friedl, M., 2018a. User guide to collection 6 modis land cover (mcd12q1 and mcd12c1) product. NASA EOSDIS Land Processes DAAC. https://lpdaac.usgs.gov/sites/default/files/public/product_documentation/mcd12_user_guide_v6.pdf.
Sulla-Menashe, D., Friedl, M., 2018b. User guide to collection 6 modis land cover (mcd12q1 and mcd12c1) product. NASA EOSDIS Land Processes DAAC. https://doi.org/10.5067/MODIS/MCD12Q1.006.
Van Vliet, N., Adams, C., Vieira, I.C.G., Mertz, O., 2013. Slash and burn" and "shifting" cultivation systems in forest agriculture frontiers from the brazilian amazon. Soc. Nat. Resour. 26, 1454–1467.
Venables, W.N., Ripley, B.D., 2002. Modern Applied Statistics with S, fourth ed. Springer, New York. iSBN 0-387-95457-0. http://www.stats.ox.ac.uk/pub/MASS4.
Ver Hoef, J.M., Boveng, P.L., 2007. Quasi-Poisson vs. Negative binomial regression: how should we model overdispersed count data? Ecology 88, 2766–2772. https://doi.org/10.1890/07-0043.1.
Wood, S.N., 2004. Stable and efficient multiple smoothing parameter estimation for generalized additive models. J. Am. Stat. Assoc. 99, 673–686.
Wood, S.N., 2011. Fast stable restricted maximum likelihood and marginal likelihood estimation of semiparametric generalized linear models. J. Roy. Stat. Soc. 73, 3–36.
Wood, S., 2017. Generalized Additive Models: an Introduction with R, 2 ed. 65. Chapman and Hall/CRC, pp. 95–114. Wood, S.N., 2003. Thin-plate regression splines. Journal of the Royal Statistical Society (B).
Zuur, A.F., 2011. Mixed Effects Models and Extensions in Ecology with R. Springer.
Zuur, A.F., Saveliev, A.A., Ieno, E.N., 2014. A Beginner's Guide to Generalised Additive Mixed Models with R. Highland Statistics Ltd.